processes

MDPI

Article

Influence of Interfacial Tribo-Chemical and Mechanical Effect on Tribological Behaviors of TiN Film in Different Environments

Yu Cao [1,2,†], Guizhi Wu [3,*,†], Yunfeng Wang [1,*], Yongjun Li [1,2] and Huijing Xu [4]

1 School of Materials Science and Engineering, Lanzhou Jiaotong University, Lanzhou 730070, China; 18291346146@163.com (Y.C.)
2 State Key Laboratory of Solid Lubrication, Lanzhou Institute of Chemical Physics, Chinese Academy of Sciences, Lanzhou 730000, China
3 School of Mechanical Engineering, University of Leeds, Leeds LS2 9JT, UK
4 Department of Biomedical Engineering, University of Southern California, Los Angeles, CA 90089, USA
* Correspondence: g.z.wu@leeds.ac.uk (G.W.); wangyunf03@163.com (Y.W.)
† These authors contributed equally to this work.

Abstract: A series of experiments has been conducted to investigate the tribological properties of a TiN film sliding against GCr15 steel balls in ambient air, low vacuum and high vacuum environments. Various friction loads and sliding velocities were also applied. The TiN film displays a steady-state friction stage after the running-in stage in all the above environments, while the durations of running-in stages are different. The steady-state friction coefficients of the TiN film were around 0.56 in ambient air and 0.3 in the high vacuum environment (1×10^{-5} mbar). In the low vacuum (1×10^{-2} mbar) environment, a low friction coefficient (around 0.19) was attained for all the friction tests on TiN film, irrespective of the applied load and sliding velocity. In the meantime, it was noticed that the applied loads and the sliding velocities would change the duration of the running-in stage before reaching the low friction coefficient. It is revealed by the analysis of wear tracks that the metal oxides induced by the tribo-chemical effect at the friction interface play an important role in affecting the tribological behaviors of the TiN films in different environments. The Raman results show that the main component of the metal oxides is hematite (α-Fe_2O_3), and the amount of iron oxide is related to the friction environment. The composition and quantity of iron oxides produced by the interfacial tribo-chemical effect affect the tribological behavior. The results also show that the mechanical wear process at the friction interface displays a polishing effect, which would reduce the surface roughness. The mechanical wear performance varies under different loads and velocities. The tribological tests results indicate that the interfacial tribo-chemical effect and mechanical wear process should be considered together rather than individually to interpret the tribological behaviors of TiN films in different environments.

Keywords: TiN film; vacuum tribology; tribo-chemical reaction; mechanical wear

Citation: Cao, Y.; Wu, G.; Wang, Y.; Li, Y.; Xu, H. Influence of Interfacial Tribo-Chemical and Mechanical Effect on Tribological Behaviors of TiN Film in Different Environments. *Processes* **2024**, *12*, 923. https://doi.org/10.3390/pr12050923

Academic Editor: Pier Gianni Medaglia

Received: 5 April 2024
Revised: 19 April 2024
Accepted: 25 April 2024
Published: 30 April 2024

1. Introduction

Reducing friction and wear has an important impact on energy consumption, economic expenditure, and CO_2 emissions [1,2]. The most typical method for reducing friction and wear is to apply a solid lubricating film on the component surface. With the development of aerospace, metallurgy, electronics and semiconductors, components are required not only to serve in atmospheric environments but also to have excellent service lifespan in vacuum environment [3,4]. Generally, a solid lubricating film deposited on a component's surface can effectively reduce friction and wear. Solid lubricating films such as diamond-like carbon (DLC) and molybdenum disulfide (MoS_2) exhibit excellent tribological properties under vacuum conditions and ambient atmospheric conditions, such as ultra-low friction coefficients and low wear rates [4–6]. However, low hardness, poor thermal stability and sensitivity to the service environment limit its application. Titanium nitride (TiN) coatings were the first hard film to be industrialized and have been widely applied in industrial applications [7,8], such as cutting tools, decorative materials and integrated circuits, due to their unique combination of high hardness, wear resistance, excellent corrosion resistance and unique golden color [9]. Many studies have been conducted on the friction of TiN films, such as dry friction in ambient air [10], high-temperature friction [11] and oil lubrication [12].

The tribological properties of the TiN film were studied in ambient air, and several friction mechanisms involving abrasive wear, adhesive wear and oxidation wear were proposed to interpret the tribological behavior [10]. The friction mechanism of the TiN film in an atmospheric environment is complicated and depends on friction heat, the tribo-chemical reaction and the relative mechanical action of the friction pair on the interface. The vacuum environment, on the other hand, considerably eliminates the impact of gas and humidity in the atmospheric environment on friction and wear and provides a way of investigating the fundamental properties of materials that determine tribological characteristics. In our previous study, a TiN film was used to slide against a steel ball under ambient air and vacuum conditions, and the friction tests' results revealed that the friction coefficient in a vacuum was substantially lower than that in ambient air. After detailed characterization and analysis, it was determined that the low friction coefficient is due to the passivation of dangling bonds at the interface, as well as the prevention of the oxidation process and the electrostatic repulsion of N atoms in a vacuum environment [13]. To date, TiN films have been investigated mainly on microstructures for their mechanical properties [14–16], but their tribological behaviors and mechanisms in the vacuum environment are still rarely reported.

To gain a fundamental understanding of the friction of the TiN film in the vacuum environment, it is important to consider the tribo-chemistry and mechanical wear together. The friction pair is subjected to mechanical and chemical activity at the same time. The chemical action is caused by active chemicals in the environment, while the mechanical action is caused by the motions of the friction couple as a result of the applied stresses. Guo et al. investigated the friction and wear properties of Ta/Ti/TiN/Ti/DLC and Ta/Ti/TiN/TiCuN/Ti/DLC thin films in sodium bicarbonate and lactic acid solutions. They discovered that different intermediate layers of thin films and different solutions have a significant impact on friction and wear performance [17]. Cui et al. studied the influence of applied loads and gaseous atmospheres on the tribological behaviors of diamond-like carbon (DLC) films and then found that the passivation of carbon dangling bonding at the sliding interface was the primary lubrication mechanism for DLC films [18,19]. Under air conditions, the adsorption of vapor molecules from surrounding gases on the solid surface can have a significant effect on adhesion and friction [20–22]. Further, the tribological properties of a sliding surface are greatly affected by the water molecules, the active gas and the inert gas in the test environment [23,24]. Conversely, under vacuum conditions, the gas and water molecules in the vacuum environment should be greatly reduced. It was also reported that severe adhesive wear occurred on the friction surface under vacuum conditions [25,26]. On the other hand, from the perspective of mechanical action, the tribological behavior of the TiN film can be influenced by the applied load as well as the testing environment. Umair Manzoor et al. investigated the size, crystallinity and optical properties of ZnO nanoparticles (NPs) synthesized via the coprecipitate method. It was found that the synthesis temperature, nucleation time and post-synthesis heat treatment of ZnO nanoparticles all affect the sensing performance [27]. Therefore, a comprehensive tribo-chemical and mechanical analysis of the friction interface is important for understanding the tribological properties of the TiN film under a vacuum environment. The outcome will also provide significant support and scientific basis for the design, optimization and application of novel coating materials used in aerospace and harsh conditions.

In this study, a series of tribological tests for TiN films were designed in different environments, including ambient air, low vacuum and high vacuum conditions. We also applied various normal loads and sliding speeds to investigate their effects on the friction behaviors of the TiN films, which will help us to dive deeply in understanding the friction performance of TiN films in different environments. In short, this paper aims to illustrate how the environmental atmosphere, the applied normal load and sliding speed affect the friction properties of the TiN film. The underlying tribological mechanism has also been studied.

2. Experimental Details

2.1. Film Deposition

The TiN films used in this study were deposited on 304 stainless steels (flat coupons, size 30 × 30 × 2 mm, Feiyue Precision Machinery Co. Ltd., Suzhou, China) via a multi-arc ion plating machine (Flexicoat 850, Hauzer Co. Ltd., Venlo, The Netherlands). Prior to deposition of the TiN film, the 304 stainless steel substrates were ultrasonically cleared by anhydrous alcohol and acetone (Kelong Chemical Co. Ltd., Chengdu, China) and then placed on the sample holder. During the deposition of the TiN film, the chamber was evacuated up to a pressure of 4×10^{-5} mbar. To remove the oxide layer and contaminants, the substrates were cleaned by argon plasma etching for 30 min at a bias voltage of −750 V. The TiN films were deposited under a N_2 atmosphere (Ar and N_2 gas were supplied by Yulong gas Co. Ltd., Lanzhou, China), the Ti target current was 60 A, and the substrate bias was −30 V. The deposition parameters of the TiN films are shown in Table 1.

Table 1. Deposition parameters of the TiN film by multi-arc ion plating.

Item	Parameter
N_2 flow	300 sccm
Ti target current	60 A
Deposition time	3 h
Substrate bias	−30 V

2.2. Tribological Tests

The tribological tests of the TiN film were carried out by a reciprocating ball-on-disk tribometer (HVTRB vacuum tribometer, Anton Paar Co., Ltd., Graz, Austria). Sensors were applied to monitor and record the motion status and experimental parameters of the friction pair over time and, thus, to obtain accurate experimental data. The tribological experiments were conducted under air conditions, low vacuum (1×10^{-2} mbar) and high vacuum (1×10^{-5} mbar). The TiN films were slid against a GCr15 steel ball (Kangda Steel Ball Co., Ltd., Yuncheng, China) with a diameter of 6 mm. In this work, the following parameter values were used: the applied normal loads were 1 N, 3 N and 5 N; the yielding initial Hertz contact stress values were 805.8 MPa, 1162 MPa and 1378 MPa; the sliding frequencies were 1 Hz, 3 Hz and 5 Hz; the corresponding sliding velocities were 1.75 cm/s, 4.71 cm/s and 7.85 cm/s; and the stoke length was set at 5 mm. All the dry friction tests were conducted at room temperature (23 ± 2 °C) and the humidity was approximately 28 ± 3%. All the tests were repeated three times. The wear scar diameter of the GCr15 steel ball after the friction test was measured using an optical microscope, and the wear volume and the wear rate (K) of the GCr15 steel ball were calculated using the following formula:

$$h = r - \sqrt{r^2 - \frac{d^2}{4}} \tag{1}$$

$$V = \left(\frac{\pi h}{6}\right)\left(\frac{3d^2}{4}\right) + h^2 \tag{2}$$

$$K = V/(FL) \tag{3}$$

where d is the diameter of the wear scar, r is the radius of the GCr15 steel ball, V is the wear volume, L is the total sliding distance, F is the applied load and K is the wear rate.

2.3. Characterization Methods

The surface morphology of the TiN film was observed using scanning electron microscopy (SEM, Mira3, Tescan Co., Ltd., Brno, Czech), and the phase analysis of the TiN film was analyzed using the X-ray diffraction (XRD, Bruker Co., Ltd., Karlsruhe, Germany) technique with Cu-Kα radiation (λ = 1.5418 Å) in the 2θ range of 10~90°. The hardness and elastic modulus of the TiN film were determined using a nanoindentation tester (TTX-NHT2, Anton Paar Co., Ltd., Graz, Austria) with a load of 50 mN, and nine individual tests wereconducted to calculate the hardness, modulus and standard deviation. The wear tracks on the TiN film after the tribological test were studied using SEM equipped with an energy dispersive X-ray spectrometer (EDS) detector.

3. Results

3.1. General Characteristics of the Titanium Nitride (TiN) Films

The surface morphology of the as-deposited TiN film is illustrated in Figure 1a. The pits and micro particles are dispersed on the surface of the TiN film, which results from the molted droplets deposited on the TiN film during the deposition process [28]. The X-ray pattern of the TiN film with 2θ scans from 10 to 90 is shown in Figure 1b, and the diffraction pattern contains five broad peaks at 36.7, 42.6, 61.8, 74.1 and 77.9, corresponding to (1 1 1), (2 0 0), (2 2 0), (3 1 1) and (2 2 2) of TiN, respectively [13]. A nanoindentation test was used to measure the hardness and modulus of the coatings. The load–displacement curve of the TiN film is shown in Figure 1c, and the hardness and elastic modulus of the TiN film were 28.2 GPa and 467.6 GPa, respectively.

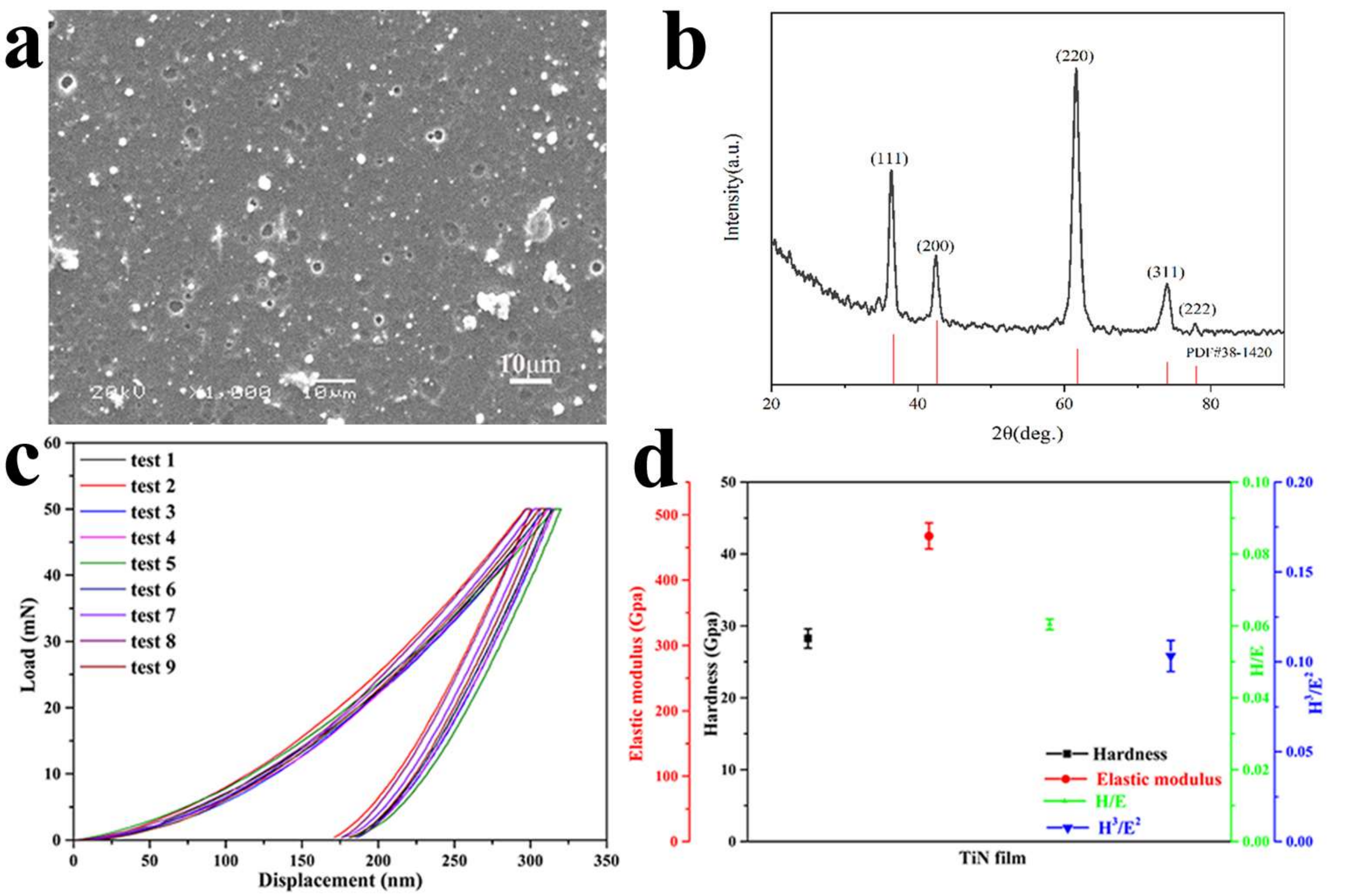

Figure 1. (**a**) SEM image of the surface morphology of the TiN film, (**b**) XRD spectrum of the TiN film, (**c**) load–displacement curve of the TiN film and (**d**) hardness and elastic modulus of the TiN film.

3.2. Friction Behavior under Ambient Air

Figure 2 shows the friction curves of the TiN film sliding against the GCr15 steel ball in ambient air with a variety of loads and sliding velocities. The friction coefficient curves of the TiN film revealed a similar trend under different experimental conditions; the friction coefficient dropped to a minimum during the running-in stage and then gradually increased throughout the test. In addition, the normal load and sliding velocity should be taken into account while analyzing the tribological behavior of the film. According to the results in Figure 2, the friction coefficient of the TiN film is affected by the sliding velocity. With the increase in the sliding velocity from 1 N–1 Hz to 1 N–5 Hz, the friction coefficient substantially decreases from approximately 0.52 to 0.41. Similarly, the friction coefficient of the TiN film was also affected by the normal load. With the increase in the load from 1 N–1 Hz to 5 N–1 Hz, the friction coefficient slightly increases from 0.52 to 0.56. Therefore, the influence of sliding velocity on the friction coefficient was greater than that of the load of the tribological properties of the TiN film in ambient air.

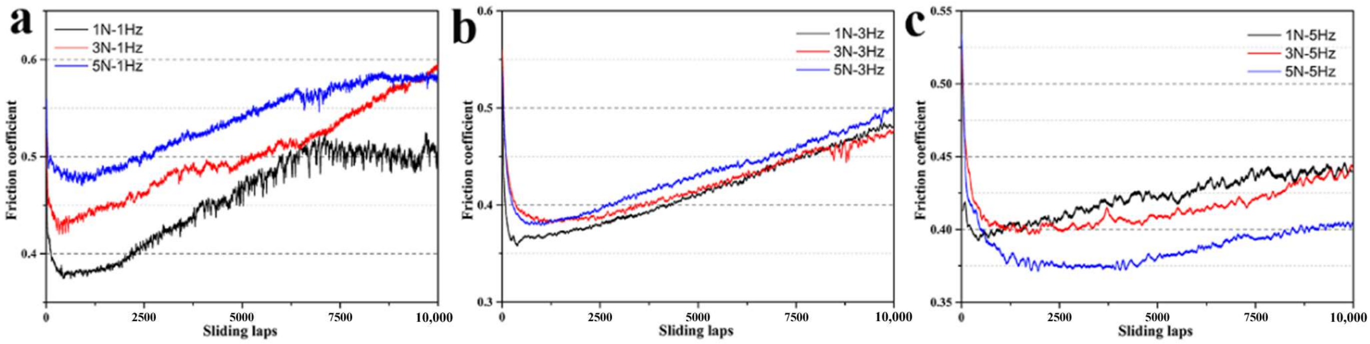

Figure 2. The friction curves of the TiN film sliding against the GCr15 steel ball under ambient air: (**a**) under various normal loads at a sliding velocity of 1 Hz (1.75 cm/s), (**b**) under various normal loads at a sliding velocity of 3 Hz (4.71 cm/s) and (**c**) under various normal loads at a sliding velocity of 5 Hz (7.85 cm/s).

The SEM micrograph and element distribution of the corresponding area of the wear tracks after the friction test are shown in Figure 3. The hardness of the TiN film (28.2 GPa) was greater than that of the counterpart GCr15 steel ball (HRC62-66). The difference in the hardness between the TiN film and GCr15 steel ball caused the material transfer of the GCr15 steel ball onto the TiN film in the friction process. As the EDS results showed, the transferred material at the friction interface was mainly composed of Fe and O elements. Moreover, it should be noted that the wear was mainly the wear of the steel balls, while the wear of the TiN film was little after the friction test. It is clear that the wear tracks on the TiN film surfaces were covered with transferred materials and abrasive particles after the friction test. The wear mechanism of the TiN film under ambient air was adhesive and abrasion wear. As seen in Figure 2, with increasing normal load and sliding velocity, the adhesive strength of the transferred material on the friction interface increases.

Furthermore, to understand the effect of the adhesive material on the friction interface, the Raman spectra of the wear tracks after the friction test of the TiN film under different normal loads and sliding velocities are shown in Figure 4. The inside (red mark) and outside (yellow mark) of the debris on wear tracks were characterized by Raman spectra, and the adhesion material was distributed in the center of the wear tracks. The composition of the inside and outside of the debris on the wear tracks was hematite (α-Fe_2O_3), and these peaks could correspond to the hematite phase (α-Fe_2O_3) [29,30].

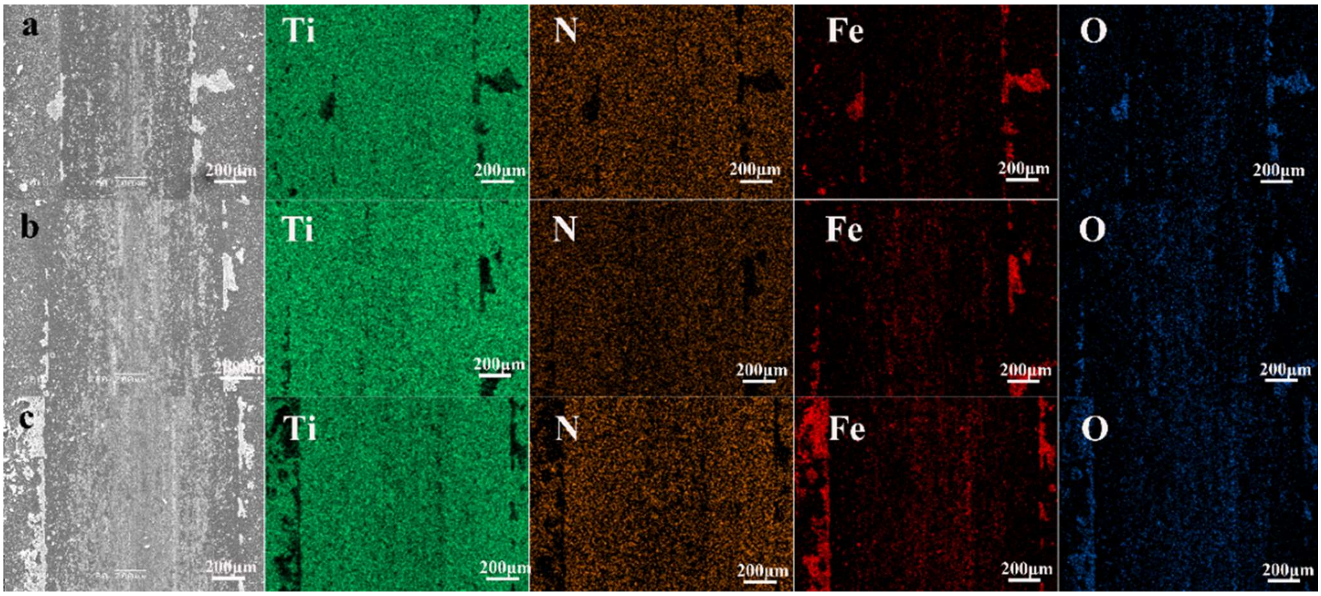

Figure 3. SEM-EDS results for the wear tracks of the TiN film after sliding against the GCr15 steel ball in ambient air: (**a**) 1 N–1 Hz, (**b**) 3 N–1 Hz and (**c**) 5 N–1 Hz.

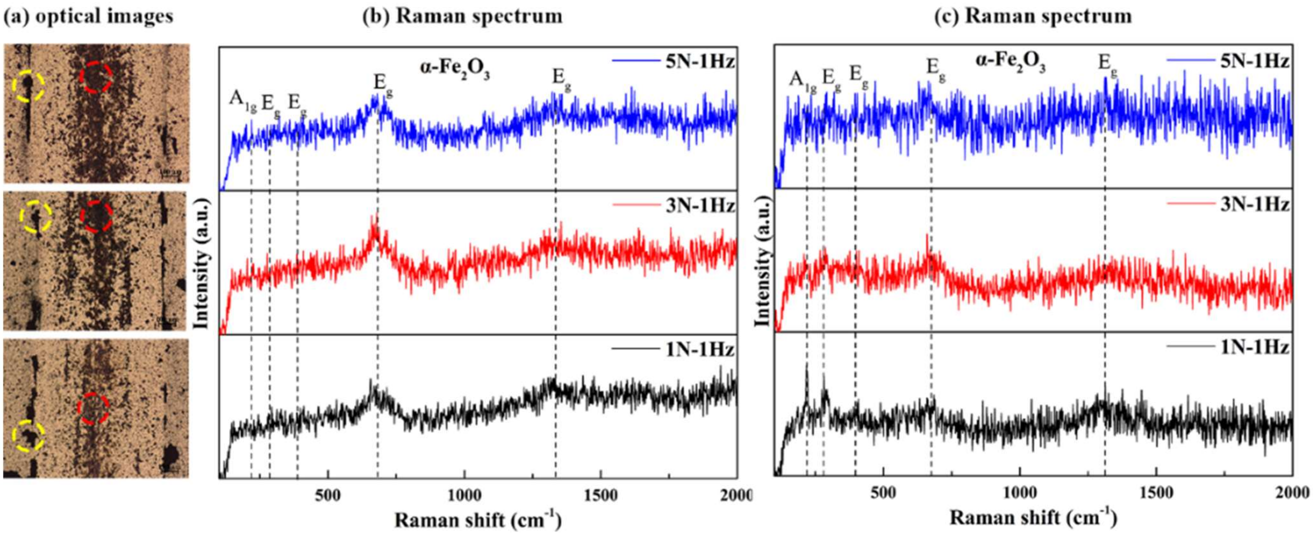

Figure 4. Optical images and Raman spectra for the wear tracks of the TiN film after sliding against the GCr15 steel ball in ambient air: (**a**) optical images of the inside (red mark) and outside (yellow mark) of the wear tracks under various normal loads at a sliding velocity of 1 Hz (1.75 cm/s), (**b**) Raman spectra of the inside of the wear tracks and (**c**) Raman spectra of the outside of the wear tracks.

3.3. Friction Behavior under High Vacuum

Figure 5 shows the variation in the friction coefficient of the TiN film under different loads and sliding velocities in a high vacuum environment (1×10^{-5} mbar). The friction coefficient decreased sharply to approximately 0.25 during the initiation to around 1000 sliding laps. Immediately, the friction coefficient increased to approximately 0.3 and remained stable through 10,000 sliding laps. Compared with the friction coefficient of the TiN film under ambient air, the friction coefficient of the TiN film under a high vacuum (0.3) was nearly half the friction coefficient of the TiN film under ambient air (0.56). In addition, the effect of the load and sliding velocity on the friction coefficient of the TiN film under a high vacuum was smaller than the friction coefficient of the TiN film under ambient air. All of the friction curves of the TiN film under a high vacuum showed a similar tendency, and compared with low load (1 N) and low sliding velocity (1 Hz), the variation range of the friction coefficient decreased under high load (5 N) and high sliding velocity (5 Hz).

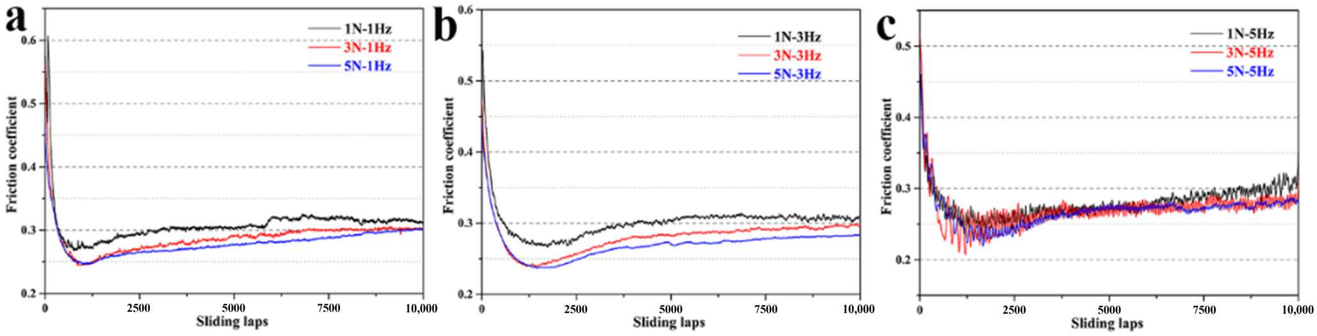

Figure 5. The friction curve of the TiN film sliding against the GCr15 steel ball under high vacuum (1×10^{-5} mbar): (**a**) under various normal loads at a sliding velocity of 1 Hz (1.75 cm/s), (**b**) under various normal loads at a sliding velocity of 3 Hz (4.71 cm/s) and (**c**) under various normal loads at a sliding velocity of 5 Hz (7.85 cm/s).

For a friction system composed of the TiN film and GCr15 steel ball, the friction behavior can be affected by the inherent properties of the TiN film and counterpart ball, the test conditions and the environmental atmosphere [31]. In this study, the diversity of friction behavior of the TiN film can be attributed to the transformation of the environmental atmosphere from ambient air to a high vacuum, and there are almost no active gases or water molecules in a high vacuum environment. Moreover, the surface chemical and physical states of the contact points have a significant effect on the tribological behavior of the TiN film during the friction process.

Figure 6 shows the SEM micrograph and element distribution of the corresponding area of the wear tracks after the friction test under a high vacuum. The wear debris produced by the GCr15 steel ball still accumulated at the edge of the wear track, but there was no obvious adhesion inside the wear track. Under the condition of a high vacuum, the gas content and humidity are very low, and the effect of tribo-chemical action can be ignored. The main contribution to the friction coefficient is mechanical wear in the interface. Compared with the wear track in ambient air, the inside of the wear track is obviously different after the friction test under a high vacuum. The inside regions of the wear tracks were very clear, indicating no adhesion between the contacting surfaces. Adhesion wear on the friction interface can lead to a large friction coefficient. This might be the reason that the low friction coefficient of the TiN film occurred in a high vacuum.

The Raman spectra obtained from the wear tracks on the TiN film under a high vacuum are shown in Figure 7. The inside (red mark) and outside (yellow mark) of the debris on wear tracks were characterized by Raman spectra. However, there is no obvious transfer of material from the GCr15 steel ball at the center of the wear tracks. The composition of the inside of the debris was titanium nitride (TiN), and the Raman peaks appeared at 209 cm^{-1} (TA), 330 cm^{-1} (LA) and 547 cm^{-1} (TO). These peaks could correspond to the titanium nitride phase (TiN) [32,33]. In contrast, the composition of the outside of the debris on the wear tracks was hematite (α-Fe_2O_3). The Raman peaks appeared at 231 cm^{-1} (A_{1g}), 293 cm^{-1} (E_g),396 cm^{-1} (E_g), 672 cm^{-1} (E_g) and 1304 cm^{-1} (E_g), and these peaks could correspond to the hematite phase (α-Fe_2O_3) [29,30].

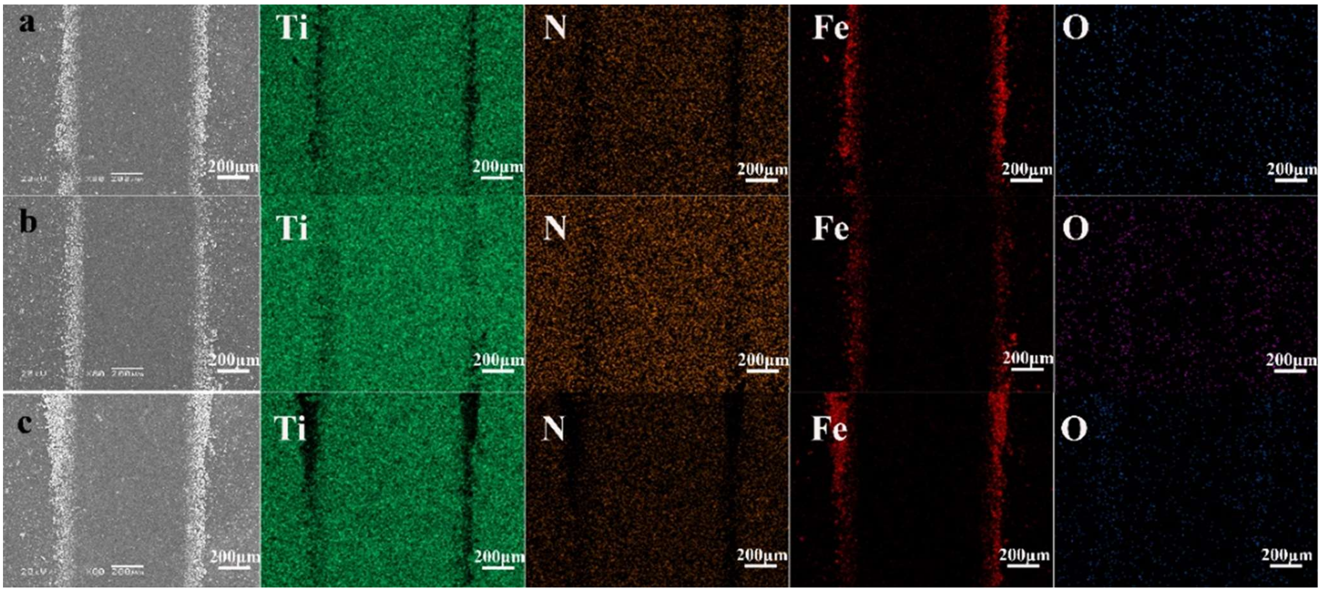

Figure 6. SEM-EDS results for the wear tracks of the TiN film after sliding against the GCr15 steel ball in a high vacuum: (**a**) 1 N–1 Hz, (**b**) 3 N–1 Hz and (**c**) 5 N–1 Hz.

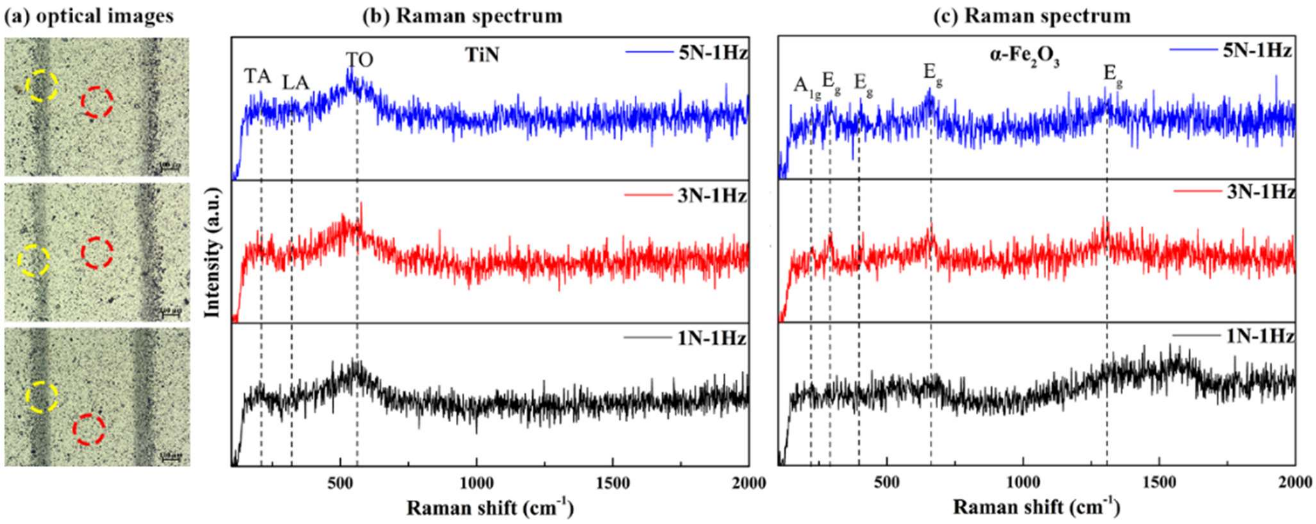

Figure 7. Optical images and Raman spectra for the wear tracks of the TiN film after sliding against the GCr15 steel ball in high vacuum: (**a**) optical images of the inside (red mark) and outside (yellow mark) of the wear tracks under various normal loads at a sliding velocity of 1 Hz (1.75 cm/s), (**b**) Raman spectra of the inside of the wear tracks and (**c**) Raman spectra of the outside of the wear tracks.

3.4. Friction Behavior under Low Vacuum

Figure 8 shows the variation in the friction coefficient of the TiN film for different loads and sliding velocities under a low vacuum (1×10^{-2} mbar). Generally, all of the friction coefficients of the curves can be divided into three stages, and the friction coefficient finally stabilizes at a value of approximately 0.2. In the first stage, the friction coefficient drops sharply to a value of 0.35 and then slowly increases to a value of 0.4 at the second stage. In the subsequent third stage, the friction coefficient drops sharply to approximately 0.2, where it remains constant throughout the entire test. However, it should be noted that the friction coefficient in a low vacuum is lower than the friction coefficient in ambient air and a high vacuum.

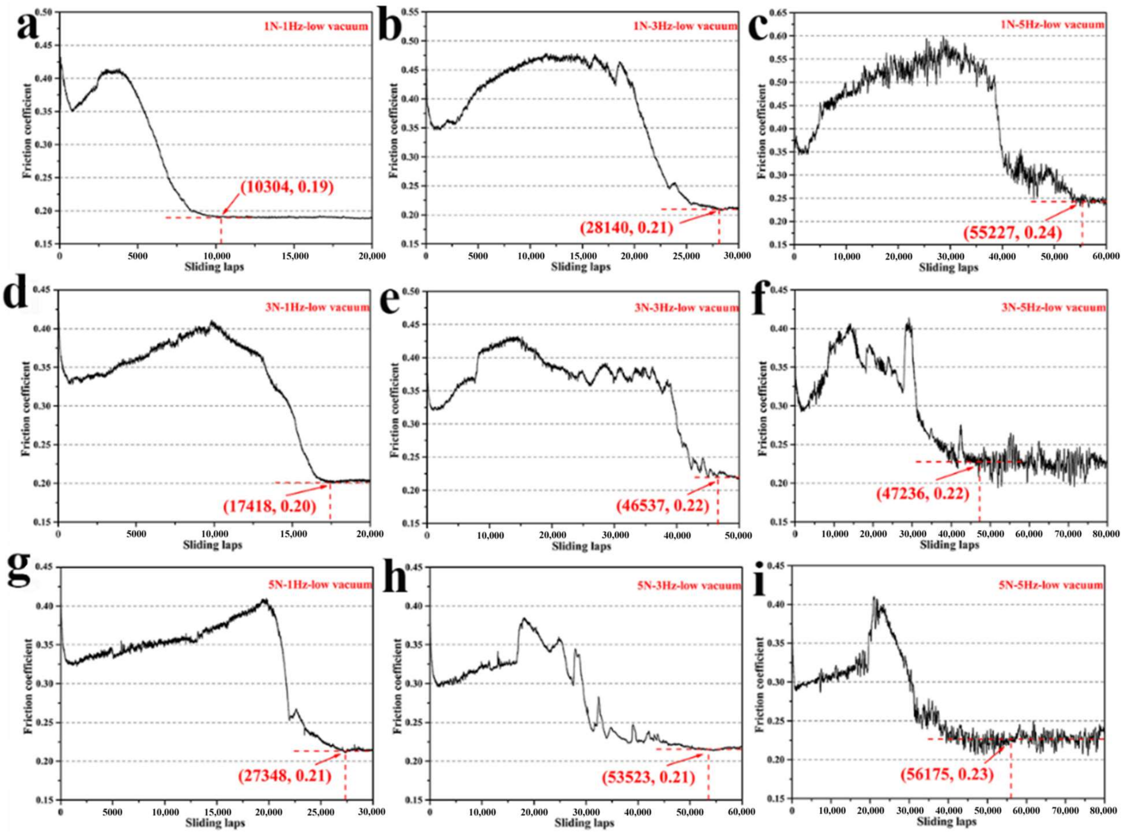

Figure 8. Friction curve of the TiN film sliding against the GCr15 steel ball under low vacuum (1×10^{-2} mbar): (**a**,**d**,**g**) under various normal loads at a sliding velocity of 1 Hz (1.75 cm/s), (**b**,**e**,**h**) under various normal loads at a sliding velocity of 3 Hz (4.71 cm/s), and (**c**,**f**,**i**) under various normal loads at a sliding velocity of 5 Hz (7.85 cm/s).

In addition, it should also be noted that the sliding laps that reach a low friction coefficient are different. The sliding laps reaching a low friction coefficient at different sliding velocities and loads are shown in Table 2. Running-in is the initial stage of sliding wear before forming conformal sliding contact, and severe wear occurs in this stage. The influence of mechanical wear on the friction coefficient is much greater than that of the tribo-chemical reaction. With the increase in the applied load and sliding velocity, the running-in period required for the friction interface to reach the stable stage is longer [34,35]. After the severe wear of the steel ball in the running-in period, the friction interface is relatively stable. At the stage of low friction coefficient, the tribo-chemical reaction plays a major role in the friction coefficient. Moreover, the contribution of tribo-chemistry to the friction coefficient continued until the end of the friction test.

Table 2. Sliding laps reaching a low friction coefficient at different sliding velocities and loads.

Experimental Parameters	Laps	Friction Coefficient
1 N–1 Hz	10,304	0.19
1 N–3 Hz	28,140	0.20
1 N–5 Hz	55,227	0.24
3 N–1 Hz	17,418	0.20
3 N–3 Hz	45,637	0.22
3 N–5 Hz	47,236	0.22
5 N–1 Hz	27,348	0.21
5 N–3 Hz	53,523	0.21
5 N–5 Hz	56,175	0.23

Figure 9 shows the SEM micrograph and element distribution of the corresponding area of the wear tracks after the friction test under a low vacuum. The wear debris produced by the GCr15 steel ball still accumulates at the edge of the wear tracks, and the amount of wear debris increases as the load increases. There is a small amount of wear debris on the inside of the wear tracks. The main component of wear debris was iron oxide.

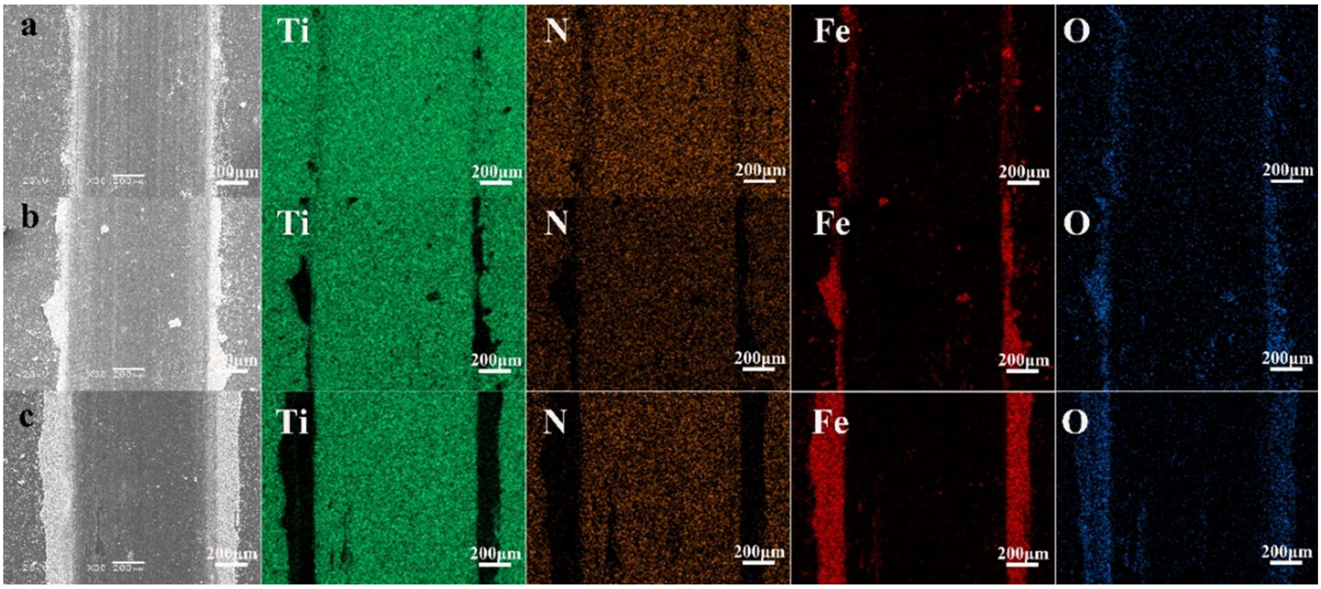

Figure 9. SEM-EDS results for the wear tracks of the TiN film after sliding against the GCr15 steel ball in a low vacuum: (**a**) 1 N–1 Hz, (**b**) 3 N–1 Hz and (**c**) 5 N–1 Hz.

The Raman spectra obtained from the wear tracks on the TiN film under a high vacuum are shown in Figure 10. The inside (red mark) and outside (yellow mark) of the debris on wear tracks were characterized by Raman spectra. The composition of the inside and outside of the debris on the wear tracks was hematite (α-Fe_2O_3). The Raman peaks appeared at 231 cm^{-1} (A_{1g}), 293 cm^{-1} (E_g),396 cm^{-1v}(E_g), 672 cm^{-1} (E_g) and 1304 cm^{-1} (E_g), and these peaks could correspond to the hematite phase (α-Fe_2O_3) [29,30].

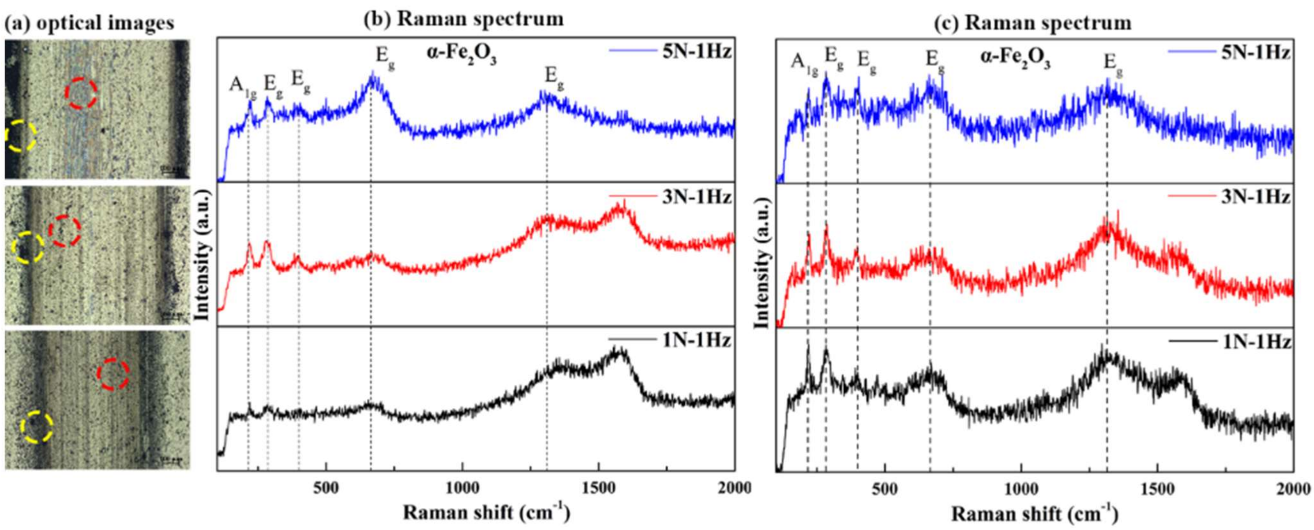

Figure 10. Optical images and Raman spectra for the wear tracks of the TiN film after sliding against the GCr15 steel ball in a low vacuum: (**a**) optical images of the inside (red mark) and outside (yellow mark) of the wear tracks under various normal loads at a sliding velocity of 1 Hz (1.75 cm/s), (**b**) Raman spectra of the inside of the wear tracks and (**c**) Raman spectra of the outside of the wear tracks.

4. Discussion

In Figure 11a, the friction results of the TiN film from different environments are summarized and presented as a function of loads and sliding velocities. In ambient air, a higher friction coefficient was observed as compared with the high vacuum environment. The different friction coefficients were related to the real contact state of the friction interface in different environments [31,36]. The wear tracks and Raman analysis showed that the mechanical wear and tribo-chemical reaction were different, where more metal oxide and adhesive wear was observed as compared with the high vacuum environment (Figure 4). In the high vacuum environment, low friction coefficients of all tribological tests were observed. The wear tracks and Raman analysis showed that no metal oxide was observed on the inside of the sliding interface (Figure 7). Tribo-chemistry has no effect on friction coefficient of the TiN film under a high vacuum. Obviously, in the low vacuum environment, the lowest friction coefficient of the TiN film was observed. It is worth noting that the lowest friction coefficient in a low vacuum was achieved by a long running-in period. Results from the present study suggest that the friction mechanisms of TiN film under different environments are different.

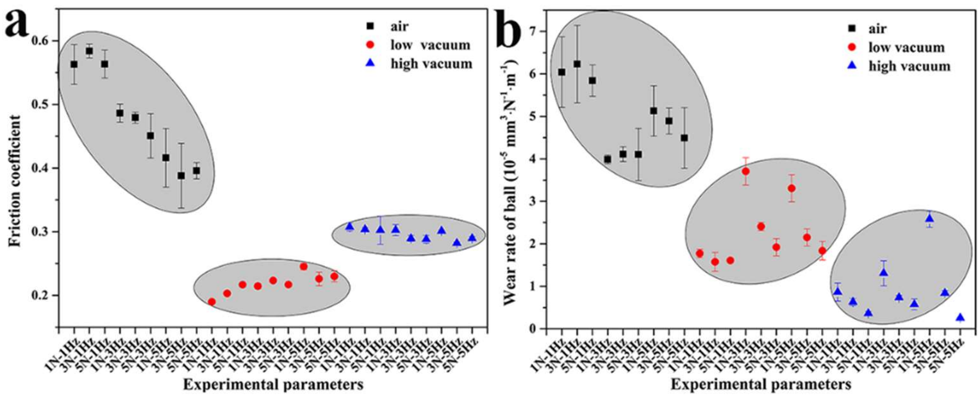

Figure 11. (**a**) Average steady-state friction coefficient of the TiN film and (**b**) wear rate of the GCr15 steel ball after friction testing under different loads and sliding velocities in ambient air, low vacuum and high vacuum environments.

The effects of friction environments on the tribological properties of the contact interface have been extensively studied [31,37]. In this study, it is worth noting that the TiN film siding against the GCr15 steel ball has almost no wear after the friction test. In Figure 11b, wear results of the GCr15 steel ball from different environments are summarized and presented as a function of loads and sliding velocities. The wear rate of the GCr15 steel ball in ambient air is higher than that in a high vacuum. The number of sliding laps used in the wear rate under a low vacuum was the same as that measured in ambient air and a high vacuum, which was 10,000 laps. As seen from the friction coefficient curves in Figure 8, a high friction coefficient stage of the TiN film in a low vacuum appeared in the running-in period. Generally, the high wear rate of the GCr15 steel ball corresponds to the high friction coefficient of the TiN film.

The friction and wear results described above raise an interesting and important question: why do the friction and wear results differ in ambient air, low vacuum and high vacuum conditions? The wear loss of material is usually estimated using Archard's wear equation, and Archard's relationship states that the wear of material is linearly proportional to the normal load and sliding distance but inversely proportional to the hardness of the materials [38,39]. Therefore, the mechanical properties of the TiN film and GCr15 steel ball dictate the wear process, and the wear of the GCr15 steel ball varies depending on the difference in the friction environment. The above results revealed different tribo-chemical reactions in ambient air, low vacuum and high vacuum environments.

The environmental atmosphere may significantly affect the tribological behavior of ceramic materials, and the friction interface after a tribological test is an important aspect that affects the friction behaviors of ceramic films [10,40]. The wear tracks of the TiN film after the tribological test in different environments are shown in Figure 12. The interfacial bond between the metal and the ceramic is generally stronger than the cohesive bond of the metal, so the metal was sheared and experienced serious wear during sliding. From Figure 12(a1,a2), it can be observed that serious adhesive wear occurred on the wear track of the TiN film in ambient air, and the serious adhesion wear of the wear track led to high friction resistance on the tribology interface. As seen in the Raman spectra in Figure 4, the transferred material inside and outside the wear tracks of the TiN film after the friction test was composed of a large amount of hematite (α-Fe_2O_3). Adhesion occurred at the tribology interface during the friction process, causing cold welding, high friction and high wear [38,41]. Therefore, the TiN film has high friction in ambient air.

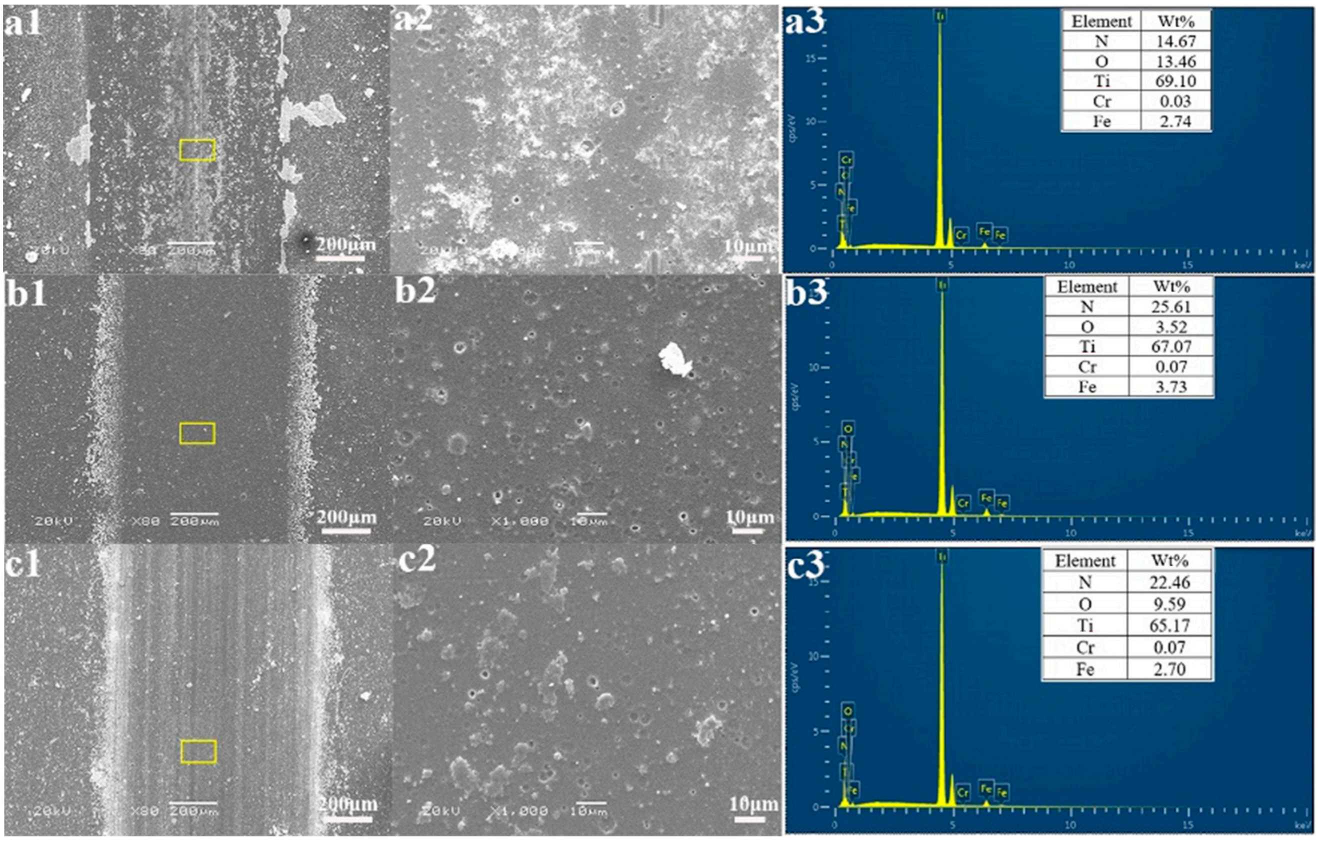

Figure 12. SEM and EDS images of the wear tracks on the TiN film after the friction test. (**a1**) SEM image of the wear track in ambient air, (**a2**) the high-resolution SEM images of the area marked with the yellow solid square in (**a1**,**a3**) the EDS images of the wear tracks in (**a1**). Correspondingly, the SEM and EDS images of the wear tracks in a high vacuum are in (**b1**–**b3**), and the SEM and EDS images of the wear tracks in a low vacuum are in (**c1**–**c3**).

From the previous friction test in a high vacuum, the friction coefficients measured in the high vacuum are all lower than those measured in ambient air. As seen in Figure 12(b1,b2), no adhesion wear exists inside the wear track of the TiN film, but there is a small amount of wear debris on the outside of the wear tracks after the friction test. As seen in the Raman spectra in Figure 7, the transferred material outside the wear tracks of the TiN film after the friction test was composed of hematite (α-Fe_2O_3), but the wear tracks were still the TiN film itself. Removing the influence of the environmental atmosphere in ambient air has enabled a better understanding of the friction interface that influences friction and wear in a high vacuum. No adhesive wear occurs at the friction interface under a high vacuum (Figure 7), and the significant wear reduction of the GCr15 steel ball was observed in the high vacuum environment (Figure 11b). This indicates that in the high vacuum environment, tribo-chemical reactions and tribo-mechanical wear on the friction interface were suppressed in comparison with ambient air. Therefore, the TiN film has low friction in a high vacuum.

From the friction coefficient curves in a low vacuum in Figure 8, the lowest friction efficient (0.19) can be achieved when the load is 1 N and the sliding velocity is 1 Hz, and the lowest friction can be achieved at different loads and sliding velocities. The wear track of the TiN film is shown in Figure 12(c1,c2). It is clear that the amount of metal oxide inside the wear track in low vacuum environments was less than in ambient air. Slight adhesion was distributed inside the wear track of the TiN film, and the transferred material inside the wear track was hematite (α-Fe_2O_3) according to Figure 10. Therefore, slight adhesion and a small amount of hematite (α-Fe_2O_3) on the friction interface can further reduce the friction coefficient.

5. Conclusions

In this study, the influence of the environment, normal load and sliding velocity on the friction behaviors in TiN films were investigated. Tribological tests were conducted on TiN film in ambient air, low vacuum and high vacuum. The following conclusions can be drawn:

(1) The friction coefficient of the TiN film was approximately 0.56 in ambient air and 0.3 in a high vacuum (1×10^{-5} mbar). The lowest friction coefficient (0.19) appeared in a low vacuum (1×10^{-2} mbar). It is worth noting that the TiN film possesses excellent wear resistance under different environments.

(2) Under ambient air conditions, a large number of active gases and humidity exist, and serious adhesive wear and abrasive wear occur at the friction interface, resulting in an increased friction coefficient. Under high vacuum conditions, there are almost no active gases or water molecules, and the friction coefficient is mainly affected by mechanical wear. Under low vacuum conditions, the tribo-chemical reaction and mechanical wear play simultaneous roles in further reducing the friction coefficient.

(3) It was observed that the tribo-chemical products (Fe_2O_3) detected by Raman and slight wear on the friction interface can define the low friction behavior of the TiN film in a low vacuum environment. Furthermore, a connection between the low friction of the TiN film and the tribological interface evolution was established by changing the friction environment. The analysis of the friction coefficient and sliding interface after the friction test in different environments reveals that the tribo-chemical reaction and mechanical wear on the sliding interface have a significant impact on the friction of the TiN film. The outcome provides significant support and scientific basis for the design, optimization, and application of novel coating materials used in aerospace.

Author Contributions: Conceptualization, G.W. and Y.L.; methodology, Y.C.; software, Y.L.; validation, Y.C. and Y.L.; resources, Y.W. and G.W.; data curation, Y.L.; writing—original draft preparation, Y.C. and Y.L.; writing—review and editing, G.W. and H.X.; visualization, Y.C.; supervision, G.W. and Y.W.; project administration, Y.W.; funding acquisition, Y.W. All authors have read and agreed to the published version of the manuscript.

Funding: This work was supported by the National Natural Science Foundation of China [grant number 52165023] and the Sichuan Science and Technology Program [No. 2019YFSY0012].

Data Availability Statement: Data are contained within the article.

Conflicts of Interest: The authors declare no conflicts of interest.

References

1. Holmberg, K.; Erdemir, A. Influence of tribology on global energy consumption, costs and emissions. *Friction* **2017**, *5*, 263–284. [CrossRef]

2. Holmberg, K.; Erdemir, A. The impact of tribology on energy use and CO_2 emission globally and in combustion engine and electric cars. *Tribol. Int.* **2019**, *135*, 389–396. [CrossRef]
3. Ando, Y.; Abe, S. Friction and wear properties of nanostripe-inducing structures in vacuum environment. *Wear* **2019**, *424–425*, 62–69. [CrossRef]
4. Xu, J.; He, T.; Chai, L.; Qiao, L.; Zhang, X.; Wang, P.; Liu, W.J.P.C.C.P. Selective-releasing-affected lubricant mechanism of a self-assembled MoS 2/Mo–S–C nanoperiod multilayer film sliding in diverse atmospheres. *Phys. Chem. Chem. Phys.* **2017**, *19*, 8161–8173. [CrossRef] [PubMed]
5. Arenas, M.A.; Ahuir-Torres, J.I.; García, I.; Carvajal, H.; de Damborenea, J. Tribological behaviour of laser textured Ti6Al4V alloy coated with MoS_2 and graphene. *Tribol. Int.* **2018**, *128*, 240–247. [CrossRef]
6. Li, P.; Ju, P.; Ji, L.; Li, H.; Liu, X.; Chen, L.; Zhou, H.; Chen, J. Toward Robust Macroscale Superlubricity on Engineering Steel Substrate. *Adv. Mater.* **2020**, *32*, 2002039. [CrossRef]
7. PalDey, S.; Deevi, S.C. Single layer and multilayer wear resistant coatings of (Ti,Al)N: A review. *Mater. Sci. Eng. A* **2003**, *342*, 58–79. [CrossRef]
8. Hsieh, J.H.; Liang, C.; Yu, C.H.; Wu, W. Deposition and characterization of TiAlN and multi-layered TiN/TiAlN coatings using unbalanced magnetron sputtering. *Surf. Coat. Technol.* **1998**, *108–109*, 132–137. [CrossRef]
9. Santecchia, E.; Hamouda, A.M.S.; Musharavati, F.; Zalnezhad, E.; Cabibbo, M.; Spigarelli, S. Wear resistance investigation of titanium nitride-based coatings. *Ceram. Int.* **2015**, *41*, 10349–10379. [CrossRef]
10. Yan, Z.; Jiang, D.; Gao, X.; Hu, M.; Wang, D.; Fu, Y.; Sun, J.; Feng, D.; Weng, L. Friction and wear behavior of TiN films against ceramic and steel balls. *Tribol. Int.* **2018**, *124*, 61–69. [CrossRef]
11. Wilson, S.; Alpas, A. Dry sliding wear of a PVD TiN coating against Si_3N_4 at elevated temperatures. *Surf. Andcoatings Technol.* **1996**, *86–87*, 75–81. [CrossRef]
12. Fu, X.; Cao, L.; Qi, C.; Wan, Y.; Xu, C. Ultralow friction of PVD TiN coating in the presence of glycerol as a green lubricant. *Ceram. Int.* **2020**, *46*, 24302–24311. [CrossRef]
13. Chen, Q.; Wu, G.; Li, D.; Li, A.; Shang, L.; Lu, Z.; Zhang, G.; Wu, Z.; Tian, G. Understanding the unusual friction behavior of TiN films in vacuum. *Tribol. Int.* **2019**, *137*, 379–386. [CrossRef]
14. Łępicka, M.; Grądzka-Dahlke, M.; Pieniak, D.; Pasierbiewicz, K.; Kryńska, K.; Niewczas, A. Tribological performance of titanium nitride coatings: A comparative study on TiN-coated stainless steel and titanium alloy. *Wear* **2019**, *422–423*, 68–80. [CrossRef]
15. Kumar, D.D.; Kumar, N.; Kalaiselvam, S.; Dash, S.; Jayavel, R. Micro-tribo-mechanical properties of nanocrystalline TiN thin films for small scale device applications. *Tribol. Int.* **2015**, *88*, 25–30. [CrossRef]
16. Wang, J.; Yazdi, M.A.P.; Lomello, F.; Billard, A.; Kovács, A.; Schuster, F.; Guet, C.; White, T.J.; Sanchette, F.; Dong, Z. Influence of microstructures on mechanical properties and tribology behaviors of TiN/TiXAl1−XN multilayer coatings. *Surf. Coat. Technol.* **2017**, *320*, 441–446. [CrossRef]
17. Guo, D.; Zhang, S.; Wu, S.; Huang, T.; Ma, X.; Guo, F. Design of an Ultra-Thick Film and Its Friction and Wear Performance under Different Working Conditions. *Coatings* **2023**, *13*, 1173. [CrossRef]
18. Cui, L.; Lu, Z.; Wang, L. Environmental effect on the load-dependent friction behavior of a diamond-like carbon film. *Tribol. Int.* **2015**, *82*, 195–199. [CrossRef]
19. Cui, L.; Lu, Z.; Wang, L. Probing the low-friction mechanism of diamond-like carbon by varying of sliding velocity and vacuum pressure. *Carbon* **2014**, *66*, 259–266. [CrossRef]
20. Marino, M.J.; Hsiao, E.; Chen, Y.; Eryilmaz, O.L.; Erdemir, A.; Kim, S.H. Understanding Run-In Behavior of Diamond-Like Carbon Friction and Preventing Diamond-Like Carbon Wear in Humid Air. *Langmuir* **2011**, *27*, 12702–12708. [CrossRef]
21. Yang, M.; Marino, M.J.; Bojan, V.J.; Eryilmaz, O.L.; Erdemir, A.; Kim, S.H. Quantification of oxygenated species on a diamond-like carbon (DLC) surface. *Appl. Surf. Sci.* **2011**, *257*, 7633–7638. [CrossRef]
22. Wu, X.; Ohana, T.; Nakamura, T.; Tanaka, A. Gaseous Tribochemical Products of Hydrogenated DLC Film and Stainless Steel Pair in Air Detected by Mass Spectrometry. *Tribol. Lett.* **2015**, *57*, 5. [CrossRef]
23. He, X.; Pollock, A.; Kim, S.H. Effect of Gas Environment on Mechanochemical Reaction: A Model Study with Tribo-Polymerization of α-Pinene in Inert, Oxidative, and Reductive Gases. *Tribol. Lett.* **2019**, *67*, 25. [CrossRef]
24. Nakayama, K.; Martin, J.-M. Tribochemical reactions at and in the vicinity of a sliding contact. *Wear* **2006**, *261*, 235–240. [CrossRef]
25. Kumar, D.D.; Rani, R.; Kumar, N.; Panda, K.; Kirubaharan, A.M.K.; Kuppusami, P.; Baskaran, R. Tribochemistry of TaN, TiAlN and TaAlN coatings under ambient atmosphere and high-vacuum sliding conditions. *Appl. Surf. Sci.* **2020**, *499*, 143989. [CrossRef]
26. Niu, M.; Zhang, X.; Chen, J.; Yang, X. Friction and wear properties of Ni3Si alloy under different vacuum conditions. *Vacuum* **2019**, *161*, 443–449. [CrossRef]
27. Manzoor, U.; Tuz Zahra, F.; Rafique, S.; Moin, M.T.; Mujahid, M. Effect of Synthesis Temperature, Nucleation Time, and Postsynthesis Heat Treatment of ZnO Nanoparticles and Its Sensing Properties. *J. Nanomater.* **2015**, *2015*, 189058. [CrossRef]
28. Shukla, K.; Rane, R.; Alphonsa, J.; Maity, P.; Mukherjee, S. Structural, mechanical and corrosion resistance properties of Ti/TiN bilayers deposited by magnetron sputtering on AISI 316L. *Surf. Coat. Technol.* **2017**, *324*, 167–174. [CrossRef]
29. Mukhtar, A.; Cao, X.-M.; Mehmood, T.; Wang, D.-S.; Wu, K.-M. Structural characterization of self-assembled chain like Fe-FeOx Core shell nanostructure. *Nanoscale Res. Lett.* **2019**, *14*, 308. [CrossRef] [PubMed]
30. Hanesch, M. Raman spectroscopy of iron oxides and (oxy)hydroxides at low laser power and possible applications in environmental magnetic studies. *Geophys. J. Int.* **2009**, *177*, 941–948. [CrossRef]

31. Velkavrh, I.; Ausserer, F.; Klien, S.; Brenner, J.; Forêt, P.; Diem, A. The effect of gaseous atmospheres on friction and wear of steel–steel contacts. *Tribol. Int.* **2014**, *79*, 99–110. [CrossRef]
32. de Sousa, R.R.M.; Sato, P.S.; Viana, B.C.; Alves, C.; Nishimoto, A.; Nascente, P.A.P. Cathodic cage plasma deposition of TiN and TiO_2 thin films on silicon substrates. *J. Vac. Sci. Technol. A Vac. Surf. Film.* **2015**, *33*, 041502. [CrossRef]
33. Chen, Q.; Li, A.; Wu, G.; Lu, Z.; Zhang, G.; Tian, G. Structure vs chemistry: Tribological behavior of TiN films in the nitrogen atmosphere. *Ceram. Int.* **2020**, *46*, 28053–28063. [CrossRef]
34. Khonsari, M.M.; Ghatrehsamani, S.; Akbarzadeh, S. On the running-in nature of metallic tribo-components: A review. *Wear* **2021**, *474-475*, 203871. [CrossRef]
35. Luo, Q. Origin of Friction in Running-in Sliding Wear of Nitride Coatings. *Tribol. Lett.* **2009**, *37*, 529–539. [CrossRef]
36. Velkavrh, I.; Ausserer, F.; Klien, S.; Voyer, J.; Ristow, A.; Brenner, J.; Forêt, P.; Diem, A. The influence of temperature on friction and wear of unlubricated steel/steel contacts in different gaseous atmospheres. *Tribol. Int.* **2016**, *98*, 155–171. [CrossRef]
37. Reichelt, M.; Cappella, B. Influence of relative humidity on wear of self-mated 100Cr6 steel. *Wear* **2020**, *450-451*, 203239. [CrossRef]
38. Scharf, T.W.; Prasad, S.V. Solid lubricants: A review. *J. Mater. Sci.* **2012**, *48*, 511–531. [CrossRef]
39. Archard, J.F. Contact and Rubbing of Flat Surfaces. *J. Appl. Phys.* **1953**, *24*, 981–988. [CrossRef]
40. Kumar, S.; Maity, S.R.; Patnaik, L. Effect of tribological process parameters on the wear and frictional behaviour of Cr-(CrN/TiN) composite coating: An experimental and analytical study. *Ceram. Int.* **2021**, *47*, 16018–16028. [CrossRef]
41. Costa, H.L.; Oliveira Junior, M.M.; de Mello, J.D.B. Effect of debris size on the reciprocating sliding wear of aluminium. *Wear* **2017**, *376–377*, 1399–1410. [CrossRef]